STATUS REPORT #2

June 1, 1965 through February 28, 1966

NGR 47-002-004

Medical College of Virginia
Richmond, Va. 23219

Department of Radiology
(E. Richard King, M.D., Chairman)

Radiation Physics Division

STATUS REPORT

FOR

PERIOD JUNE 1, 1965 THROUGH FEBRUARY 28, 1966

on

NASA Grant NGR 47-002-004*

(Investigation of total energy absorption in
omnidirectional gamma-ray, Bremsstrahlung and neutron fluxes)

Fearghus T. O'Foghludha, Ph.D.
Principal Investigator

March 28, 1966

*Office of Advanced Research and Technology, Division of Biotechnology and Human Research

1. Introduction:

The status report[+] submitted June 24, 1965 described the initial phases of work begun (nominally) January 1, 1965, under four headings there numbered as follows:

2. Spectral measurements

3. Chemical investigations

4. Omnidirectional irradiation

5. Sundry investigations

Further studies under each heading are now reported.

2. Spectral Measurements:

The previous submission outlined the well-known matrix inversion method of "unscrambling" complex scintillation pulse-height spectra and described the work then under way to obtain a response matrix. This work has been continued and expanded in several ways:

a) The Victoreen "SCIPP" 400-channel analyzer acquired just before submission of SR1 has been brought into relatively trouble-free operation and an entirely new set of calibration spectra (including those of the previously-unavailable Ce-141 and Sr-85 nuclides, with gamma-lines at 0.145 and 0.513 MeV, respectively*) was taken with a side-shielded but otherwise uncollimated 3" x 3" NaI(Tl) crystal; the calibration spectra previously reported were discarded because of uncertain operation of the analyzer. The sources were prepared by evaporatin

[+]Referred to in the following as SR1.

*Calibration lines are now available at 0.145, 0.279, 0.320, 0.411, 0.513, 0.662, 0.840 and 1.12 MeV and are derived from measurements made with Ce-141, Hg-203, Cr-51, Au-198, Sr-85, Cs-137, [illegible] and Zn-65.

aqueous solutions to dryness on "Mylar" film, giving essentially scatter-free conditions. All spectra were taken at constant gain; a Fluke model 413-C precision high-voltage supply was substituted for the built-in analyzer unit in order to minimize gain drift traceable to photomultiplier voltage variations.

The matrix elements were found by measuring the areas enclosed between adjacent pairs of ordinates erected at the margins of the desired energy-intervals, after normalization of the spectral area to the crystal efficiency at the calibration energy; equal ordinate separations or "bin-widths" were used in constructing this first matrix, whereas bin-widths which varied with energy were used in later versions (see Section 2(b)). Since the calibration spectra are limited in number, a good deal of interpolation is called for, the more so because of the presence of backscatter and x-ray peaks - the latter arising not only from certain calibration sources (e.g. Cs-137) but also from excitation of atoms in the crystal shield. Some simplification is introduced, however, by the fact that it is possible to obtain more line-shapes than there are nuclides by proper inter-subtraction of spectra having common lines. For example, manipulation of Rb-86, Sc-46 and Zn-65 spectra will yield the shapes of three lines - although only one of the nuclides is strictly monoenergetic - because all three exhibit a line very close to 1.1 MeV. Similarly the availability of Sr-85, which emits a gamma-ray whose energy (0.513 MeV) is for all practical purposes identical with that of annihilation radiation, permits the subtraction of annihilation contributions from the spectra of positron-emitting nuclides such as Zn-65, where the presence of the perturbing line would otherwise be troublesome.

The relatively coarse array (energy-bins 0.15 MeV wide) obtained by these techniques was inverted on the Department of Biometry's RPC-4000 computer* to yield the response matrix (M^{-1}); the product $(M)(M^{-1})$ has unit elements to one part in 10^6. Because of reconstruction work (see Section 4) on the full-size phantom manipulator described in SR1, spectra could not conveniently be taken from a man-like source and the inverse matrix was therefore applied to the study of scattering effects in an extended slab-like source which, though of simpler shape, was nevertheless big enough to simulate the maximum spectral distortion likely to be encountered in any anthropomorphic situation. The apparatus used (Fig. 1) consists of an inner polythene tank measuring 46 x 31 x 30 cm, surrounded by another measuring 62 x 46 x 45 cm. The inner tank was filled with aqueous radioactive solutions to various depths and at each depth could be surrounded with inactive or active liquids placed in the space between two tanks.

Fig. 2 shows pulse-height spectra obtained in this way, using Zn-65. The lower curve was taken from a point source in virtually scatter-free conditions, while the upper one shows the pulse-height spectrum obtained when the inner tank was filled with active solution to a depth of 25 cm. The curves are normalized to equal counts in the total absorption peak; the spectra taken at intermediate thicknesses lie between the extremes shown, with surprisingly little difference in shape for source thicknesses greater than 5 cm.

*I am indebted to Prof. S. J. Kilpatrick for providing computer time and programming services.

At first sight, the upper curve seems to indicate the presence of a large scattered-radiation component. However, even in the lower spectrum, pulses occurring below the total-absorption peak (in a region such as A) do not represent the arrival at the crystal of low-energy photons, since scatter-free conditions obtain, but are due to incomplete absorption of full-energy primaries; bearing this in mind, it is seen that pulses in region A of the degraded spectrum must result only partly from catastrophic absorption of degraded photons of that energy, the balance arising from

(a) Compton interactions (within the crystal) of undegraded photons - exactly as in the scatter-free case.

(b) Compton interactions, in the crystal, of photons whose energy was reduced to a value exceeding A during escape from the phantom.

The matrix inversion method allows these factors to be separated out, and on multiplication of the pulse-height spectrum (represented as a column matrix) with M^{-1}, the true photon spectrum shown in Fig. 3 is obtained. It is now seen that the relative contribution of scattered photons is considerably less than a first examination of the pulse-height spectrum would lead one to assume.

Knowing the energy-dependence of the counters with which the extended-source measurements are to be made, the influence of degraded photons on the response can be allowed for, since the ratio E_i/E_t of the indicated and true exposures is given by

$$\frac{E_i}{E_t} = \frac{\Sigma \mu(k)\{k \cdot N(k)\Delta k\} R(k)}{\Sigma \mu(k)\{k \cdot N(k)\Delta k\}} \qquad (1)$$

where $\mu(k)$ is the mass-absorption coefficient of air at photon energy k, $N(k)\Delta k$ is the photon fluence in an energy-interval Δk

centered about k, and R(k) is the response of the detector, defined as the reading (in exposure units) obtained when the true exposure at energy k is unity.

The counters used (see Section 4(b)) are small-volume halogen-quenched Geiger-Müller brain probes ("Selverstone" probes), air- and decane-filled ionization chambers, and an anthracene-crystal scintillation counter. Measurements of R(k) are now in progress for the G-M counters, using the air ionization chamber as an inter-comparison device; because the electrometer is capable of measuring currents over a very wide range (at least eight powers of ten) one can compare the chamber energy-response with that of NBS-calibrated x-ray chambers at high intensities, later comparing the response of the chamber with that of the G-M counters at low intensities. In this way, the energy dependence of the G-M probes (and, of course, of the ionization chamber) can be referred to NBS figures.

Although this work is not complete, it is possible to estimate the influence of spectral distribution on the G-M counter response by noting that the number of counts per roentgen as a function of photon energy is of the form shown in Fig. 4 (Sinclair, 1950) where the results for counters with two different cathode materials are given. The cathode of the Lionel type 155 probe used in the present work is made of stainless steel, whose effective atomic number lies between that of aluminum and copper, and it is therefore reasonable to assume that the counter readings will lie between those which would be obtained in the two extreme cases shown in Fig. 4. The value of E_i/E_t for a copper-cathode counter exposed to the flux of Fig. 3 is 1.03, while for an aluminum cathode it is 0.98, indicating that the effect of scattered radiation is negligible if

the spectral distortion does not appreciably exceed that shown in Fig. 3. It should be pointed out, however, that the answers obtained might be different if the summation signs of eqn. (1) were replaced by integral signs, and if the photon intensities at the lower energies were not assumed to be zero as in the present case. Presence of noise at low pulse-height has so far precluded the satisfactory measurement of photon intensities in that energy region, although the schemes referred to in sections 2(b) and 2(c) below show promise of better resolution at low k-values.

For ionization-type detectors, the usual energy characteristic is flat down to 0.1 MeV at least and thereafter rises or falls by not more than 50%. For such an energy-characteristic the ratio E_i/E_t also differs negligibly from one. The response of the anthracene pulse-counter has not been fully investigated as yet, but it follows from general arguments that spectral distortion should not seriously influence the results in this case either. It appears then that spectral distortion does not prevent reciprocity-principle measurements in the proposed geometries. The influence of scatter when a radioactive organ is surrounded by a large inactive mass remains to be investigated, and may be considerable.

b) A different data reduction scheme (Hubbell and Scofield, 1958) was also used as follows:

The system gain was varied during the measurements so that the total absorption peak of each calibration nuclide lay in the upper 1/4th of the usable pulse-height range. The spectra, automatically corrected for background and

deadtime, were normalized so that:

a) the photopeak area was the same for all spectra

b) the (calculable) pulse-heights corresponding with the Compton edges E_c were identical for all primary photon energies.

Subtraction of the photopeak from each normalized spectrum yielded a series of standard Compton continua. The shapes of continua for values of E_γ other than those used in obtaining the standards, could be constructed by interpolation. On re-addition of photopeaks (whose shapes could be synthesized at arbitrary E_γ knowing both energy-resolution and total-absorption pulse-height as a function of E_γ) to the interpolated continua, pulse-height spectra for values of E_γ centered on the proposed energy-bins could be constructed and were used, after appropriate efficiency normalization, to calculate response elements as before.

Three inverse matrices (14 x 14, 21 x 21, 42 x 42) were constructed in this way; in each matrix the bin-width was made proportional to the system resolution at mid-bin energy. Photon spectra obtained by application of the 14 x 14 and 21 x 21 matrices to the pulse-height spectrum of a water-immersed Sc-46 point source, are shown in Fig. 5. A negative photon intensity, typical of the instabilities brought about by undue narrowing of bin-widths, appears in the spectrum obtained by using the 21 x 21 array. The rather uncertain interpolations used in constructing the matrices no doubt contribute also to such false results and a means of generating monoenergetic radiation of continuously variable E_γ would be extremely valuable; methods based on selective Compton

scattering and on crystal diffraction have been proposed in a recent request for renewal of support. Equipment is also being constructed to investigate the effect of back-scatter peaks on unscrambling accuracy.

c) The unscrambling technique of Burrus, originally written for an IBM 7090 machine, has been modified for use with the IBM 1410 computer available in the Medical College. The Burrus technique, described in a number of papers (e.g. Burrus and Verbinski, 1963; Burrus, 1965), seeks to calculate the pulse output of an "ideal" analyzer, defined as one which gives a simple Gaussian distribution (unaccompanied by a Compton tail) for each gamma-ray energy. The resulting spectrum is not the required photon distribution and at first sight appears to be no more than a useful approximation to it. Burrus shows, however, that it is unprofitable to seek a more exact solution and that the greater detail of the methods already discussed is more apparent than real, being achieved at the expense of inaccuracies which finally lead to instability (as illustrated by the 21 x 21 result of Fig. 5) if more detail is sought than the analyzer is inherently capable of revealing.

The Burrus method, in essence, finds a set of coefficients which will permit the response functions of an ideal analyzer to be synthesized by combining the observed response-functions K (see SR1, page 2) of the non-ideal instrument actually used. Knowledge of the coefficients permits the calculation, within specified confidence limits, of the output which would be given by an ideal spectrometer. The calculations require the solution of a matrix equation involving three matrices (ideal, non-ideal, observed) and are no less tedious than the

normal unfolding approach, but have the advantage that oscillations are excluded and that the confidence levels are known.

In its new form, the program contains some 110 Fortran instructions and several read-in sub-routines. Operation requires modification of the computer's processor programs, since disc storage - which has not been previously used for such purposes in the College - is called for; the method will be applied to experimental spectra as soon as these changes are complete.

3. Chemical Investigations:

As stated in SR1, development of new chemical methods is not a primary objective of this project and work has been limited to the use of well-known techniques. The previous report outlined work on three variants of the Fricke-Morse dosimeter. The status of these modified ferrous-ferric systems - and of another variant using benzoic acid stabilization - is reported below; a description of another standard method (aqueous benzene system) which has been brought into use is also given.

a) Sodium thiocyanate complexing: Although the spectrophotometry of sodium thiocyanate complexes is a standard analytical method for ferric ion determination, we have found its use in dosimetry to be complicated by the formation of an interfering ferrous-ion complex and for this reason, measurements have not been taken beyond the preliminary stage reported in SR1.

b) "Tiron" complexing: The red or blue complexes formed, in basic or acid media respectively, by the organic reagent "Tiron" (disodium-1,2-dihydroxy-benzene-3,5-disulphonate) have been used by Yoe and Armstrong (1944) in extremely sensitive determinations of iron (III) (0.3 ppm) and titanium (IV)

(5×10^{-3} ppm). The exceptional dosimetric sensitivities evidenced by the visible changes observed (SR1, page 4) at dose levels of order 150 rads have proved illusory, however, since all solutions of the same composition have been found to reach the same optical density after an equilibration period of about 30 minutes, irrespective of their radiation history. The mechanism, considered plausible by Yoe (private communication) in whose original work only trace amounts of Fe(II) were present, is oxidation of Fe(II) by excess Tiron, the resulting Fe(III) then complexing with the remaining Tiron.

c) o-phenanthroline complexing: Spectrophotometry of ferrous ortho-phenanthroline complexes is, like the thiocyanate method, a standard procedure for determination of iron in trace amounts. Proposed as a detector for the Fricke-Morse system by Fortune and Mellon (1938) and developed further by Bouziges and others (1961), it has the advantage in principle that chemical after-effects (see (d) below) are avoided insofar as the quantity of unchanged ferrous ion is determined and the post-irradiation behavior of the ferric ion is of little importance because of the relatively low concentration. We have operated the system satisfactorily at high doses but at the low doses in which we are interested, the change in Fe(II) concentration is so small in comparison with the initial value that accurate measurement is impossible. Thus the method, though undoubtedly useful in the high dose range, is of little interest for the purposes of this project.

d) Ferrous sulfate-benzoic acid system: The fourth Fricke-Morse variant investigated is one employing 10^{-3} M ferrous sulfate

and 10^{-3} M benzoic acid in 1.0 N sulfuric acid. Balkwell and Adams (1960) who originated the system, report a much increased sensitivity, their measured G-value at cobalt-60 energies being 62.8 molecules/100 eV compared with 15.4 in the unmodified Fricke-Morse system; auto-oxidation is also significantly inhibited, apparently through formation of a ferrous complex. Although we have been able to detect doses of order 25 rads with ease, for both cobalt-60 gamma-rays and 300 kV x-rays, the reproducibility is poor from one exposure "run" to another and we have been unable to duplicate the $\pm$1% precision which Balkwell and Adams claim to be possible at absorbed doses of 30 rads. The linearity is excellent with no evidence of saturation up to the highest dose-levels we have employed ($\sim$ 2000 rads). Whether the sensitivity fluctuations experienced between one set of exposures and another are due to post-irradiation aging, to temperature variations or to some other cause has not yet been thoroughly investigated.

The system, in spite of the difficulties encountered, is attractive because of its sensitivity and also because it is simple to operate, requiring only a single easily-prepared distilled-water solution and a spectrophotometer set at 304 mμ.

e) Aqueous-benzene system: The well-known aqueous-benzene dosimeter described by Day, Stein and Weiss (1949) measures the absorbed energy in terms of the quantity of phenol produced during irradiation of saturated benzene solutions. The advantages of the system (Johnson and Martin, 1962) include stability, the feasibility of using relatively impure reagents and the non-corrosive nature of the solutions. The G-value -

about which there is some uncertainty - is about 2.4 molecules phenol/100 eV. The phenol is determined spectrophotometrically either directly at 595 mμ or (Klein, 1961) by using the standard analytical technique (Gibbs, 1927) of complexing with 2,6-dibromo-n-chlorobenzoquinoneimine, thereafter determining the absorbance at 650 mμ; in this method the ultimate sensitivity is reported to be about 10 rads.

Our work almost exactly duplicates Klein's technique. The irradiated benzene solution (0.021 M at 20°C) is allowed to stand for 24 hours, whereupon it is buffered at pH 9.5 and the quinoneimine reagent added. After a further 24 hours the blue complex is extracted with n-butyl alcohol and the absorbance determined. Measurements on complexes formed in phenol solutions of known concentration permit determination of the phenol liberated in the irradiated sample, from which the absorbed dose is calculable, knowing the phenol G-value.

Linearity is excellent in the low dose range examined by us (~2000 rads max) but as in the case of the ferrous-benzoic system, the reproducibility is poor. The effects of aging time, temperature, etc., are now being studied, but in general the system holds little promise for routine use because of its tedium and complexity. In this connection, the calibration of the system aginst the Fricke-Morse dosimeter is being attempted, thus giving the dose directly in terms of butyl-phase absorbance and eliminating the additional inaccuracies of phenol standard preparation.

4. Omnidirectional Irradiation:

Phantom mount: The original phantom mounting (Fig. 2 of SR1) permitted rotation about two mutually perpendicular axes only, and the

rotation speed could not be made to follow any predetermined time-pattern. These limitations precluded flux anisotropy measurements which, with the equipment then available, demanded multiple observations while the phantom successively occupied a series of accurately-known angular positions. Further, the system did not allow study of two-dimensional asymmetry (see footnote, page 15) and for these reasons an entirely new manipulator was constructed (Fig. 6).

The three-point levelling table previously used has been replaced by a quadrupod of welded steel construction, having at its center a cylindrical steel bushing in which a 4" diameter shaft is supported vertically by large ball-races. A superstructure consisting of a counterweighted carriage of 5' radius is attached to the shaft, its weight being taken by a 5" thrust bearing. This arrangement permits the carriage to rotate in azimuth ("yaw") through 360°. The carriage bears a horizontally-mounted fork of steel I-beam construction whose "handle" rotates in a sleeve provided with ball-bearings. The fork in turn supports a seat in which the REMCAL man-like phantom (see SR1, page 5) can be positioned. These arrangements permit the phantom to rotate about an axis lying in the coronal plane - a motion we shall describe as "rolling" - while sagittal rotation or "pitching" is simultaneously provided by means of a third axle mounted in bearings attached to the fork prongs. Roll and pitch movements are driven by 1/8 h.p. variable-speed DC motors, operated from phased-thyratron controls. The yawing drive was originally provided by a similar motor but even with careful balancing, variations in load during phantom rotation, coupled with excessive non-linearity of speed control at high loads, necessitated replacement by a 1/2 h.p. DC motor whose speed is varied by a silicon-controlled rectifier device.

Phantom orientation in all three planes of rotation is remotely indicated by selsyns; the repeaters are provided with resettable revolution

counters whose indication is independent of rotation sense. Drive and control leads are brought to a control panel (Fig. 7) by a slip-ring system employing 26 ring-brush pairs at the main collecting point. The manipulator is mounted in a large metal drip-tank and a mobile liquid-handling system using a peristaltic pump has been built for filling purposes. "Swagelok" quick-disconnect couplings are used - not altogether successfully - to minimize spillage. The E-detectors are supported on a track-mounted dolly providing all movements (including angling).

The phantom assembly is housed in a heavily-shielded suite designed to house a linear accelerator. Controls are situated in an adjoining room, separated from the accelerator space by a 4'-thick concrete wall with motorized safety door. A closed-circuit T.V. system incorporating a remote pan-and-tilt unit, built in the departmental shops, permits surveillance of the entire radiation area. The entire equipment was dismantled in December 1965 and re-erected at NASA-SREL in connection with the opening ceremonies there. It has since been assembled once more at the Medical College.

Since, in addition to the features described, speed-programming about any rotation axis is possible (see below) a manipulator of exceptional versatility with application in radiation therapy as well as in astronautical work, is now available. The expense of constructing it, however, has exceeded expectations and provision of the necessary shop time by an already over-extended division has also taxed available resources. Additional shop support is vital if projected changes in the drive and programming systems (see below) are to be completed in any reasonable time.

Speed programming: Determination of energy-absorption in a stationary body exposed to a zenith- (or azimuth-) dependent flux proceeds, in "reciprocal" (or conjugate) experiments, by making the residence time of the E-detector, at any given angle, proportional to the intensity which

would be observed in this orientation in the actual exposure which the inverse experiment seeks to simulate; in practice, because it is not easy to drive the E-detector over a spherical surface in the limited space available, the detector is instead held stationary while the body is rotated so that the desired pattern of relative motion is obtained. To permit investigation of virtually any angular flux-pattern, each motor can be connected to a "Data-Trak" electrostatic curve-follower which governs the speed in accordance with a graph of speed-setting vs. time. The required speed program is obtained as follows:

Suppose that the dependence of incident intensity on zenith angle* is $f(\theta)$ then the angular drive-velocity should vary as $1/f(\theta)$ if the dwell time at angle θ is to follow $f(\theta)$. To signal values of $1/f(\theta)$ to the motors, however, $1/f(\theta)$ must be known as a function of time rather than of angle. The required time-dependence is found by making use of

$$t(\theta) = \int_0^{\theta} f(\theta)\, d\theta \qquad (2)$$

where $t(\theta)$ is the time taken to reach a zenith angle θ; a signal which at time $t(\theta)$ sets the speed at $1/f(\theta)$ will drive the motors suitably. Non-linearity of the motor speed characteristic must be taken into account in plotting the curve-follower program as must the impossibility of reducing the motor speed to zero. The latter factor makes it necessary to add a constant-speed component whose contribution to the measured E-value per cycle can, however, be subtracted out in control experiments.

*Defined with respect to some arbitrary axis within the phantom. Suitable choice of reference axis permits investigation of Σ for different astronaut attitudes, while the effects of two-dimensional flux asymmetry can be studied if the phantom is rotatable about three axes, as in the present case.

The integral (2) above, always calculable numerically, is well known in certain cases. Thus for a cosine-dependent angular velocity (not flux) ω, superimposed on a constant rotation ω_o, we require to plot $(\omega_o + \omega\cos\theta)$ which is the curve-follower setting necessary to produce a motor speed $(\omega_o + \omega\cos\theta)$, versus

$$\frac{1}{\sqrt{\omega^2-\omega_o^2}} \log_e \left[\frac{\sqrt{\omega+\omega_o} + (\sqrt{\omega-\omega_o})\tan\theta/2}{\sqrt{\omega+\omega_o} - (\sqrt{\omega-\omega_o})\tan\theta/2} \right]$$

which is the time required to turn through an angle θ. Fig. 8 shows such a program for a single right-angle turn.

Poor motor regulation, the considerable inertia of the phantom carriage and the finite recycling time of the curve-follower produce errors which are cumulative - an inherent disadvantage of the time-programming method. If, for one of the reasons quoted, the angle reached at a programmed time $t(\theta)$ is $(\theta \pm \Delta\theta)$ instead of θ, then the programmer will at that instant impress a speed proportional to $1/f(\theta)$ rather than to $1/f(\theta \pm \Delta\theta)$ as required. The result is a fluctuating phase-shift which is difficult to eliminate unless very accurate speed-control is obtainable at high motor powers. For this reason, another system is being constructed, relying on servo-devices which sense the instantaneous angle and set the drive speeds accordingly.

5. Sundry Investigations:

E-detectors: Although the results obtained with the NaI(Tl) spectrometer described on page 1 are essential in interpreting the readings of the E-detectors actually used, the device itself is totally unsuitable for E-measurements because the attenuation coefficient of the crystal material changes too quickly with energy (Whyte, 1959). Three types of E-detectors have been

studied

a) Geiger-Müller probes: The energy-dependence of these probes and the influence of spectral distortion on exposure measurements made with them, have been discussed on page 5. Their principal disadvantage is the difficulty of direct calibration in fields of widely differing intensities, since the available range of count-rates is limited; for example, exposure to high-intensity x-ray fields - the only simple means at low quantum energies of relating response to that of chambers with calibrations traceable to the National Bureau of Standards - is for all practical purposes impossible. For this reason, the comparison chamber technique (page 5) is being developed.

b) Comparison chamber: After experiments with graphited-lucite chambers, which were abandoned because of unreliable electrical continuity, the metal construction shown in Figs. 9 and 12 was adopted, although the energy dependence is less favorable. The long-stem design, following that of Van Dilla, is intended to permit use with a liquid decane filling in order to increase the sensitivity (Stahel, 1929; Van Dilla, 1951) but the filling has proved unnecessary in the comparison work. The chamber is operated from a stabilized voltage supply and its output is measured by means of a Keithley Model 610B electrometer reading from the ampere range down to 10^{-14}A full-scale; a 10^{-14}A bucking source is also available. The chamber is fully saturated at 75 volts for all exposure-rates so far investigated and the response is practically independent of the angle of incidence except

within a cone of semi angle ~15° lying along the stem direction. Inverse-square behavior, which may be of importance in small-distance calibrations using low-activity nuclides, is excellent down to 20 cm; the stem current is negligible because of the guard-ring construction.

Work on the chamber energy-response, with a view to calibration of the anthracene detector (below) is proceeding.

c) Anthracene Detector: Anthracene and similar organic scintillators are known (e.g. Whyte, 1959) to give relatively energy-independent responses and in previous work (O'Foghludha, 1964) a plastic material of this type (N11/x-ray, now marketed as NE102) has been shown to be usable as an integrated-light detector down to 80 keV. The sensitivity is also excellent, a photomultiplier with an anode sensitivity of 200 A/lumen giving currents of order 10^{-8}A per mrad/hour when coupled at moderate efficiency to a cylindrical phosphor 1" long x 1/2" diameter. However, total-light observations rely on electrometric techniques and are therefore subject to drift, while time-integration and background suppression are also troublesome. For this reason the detector now to be described is operated in the pulse mode, as in the Hurst neutron dosimeter (1953).

In pulse-counter dosimetry, the energy-deposition in the crystal material - and hence the exposure at the crystal position - is found by evaluating the integral

$$\int_0^{E_{max}} E \cdot N(E)dE \qquad (3)$$

where N(E)dE is the number of interactions leading to an

energy-transfer in the range E to (E + dE). The integral can be formed from the pulse-height spectrum by scaling the analyzer clock-pulses or more simply by hand multiplication. Separate time-integration of signal and dark current pulses is now possible and subtraction of the background becomes easy - in fact, with the SCIPP analyzer, the arithmetic can be performed automatically; drift problems are also very much reduced.

Construction of the detector, which is based on an EMI 9524B 1" diameter photomultiplier working into a Victoreen preamplifier, is conventional. The anthracene crystal measures 2 cm diameter x 2 cm long approximately and is provided with a calibration window through which monoenergetic (internal conversion) electrons can be admitted. Typical signal and background spectra are shown in Figs. 10(a) and (b).

Calibration of the detector against NBS-certified chambers is now underway. The influence of phosphor composition and shape will be investigated in the near future.

d) Scatter integrals: In SR1 (page 6) an account was given of comparisons made between the Meredith-Neary (1944), O'Foghludha (1959) and Carlsson (1963) methods of energy determination, and a new formulation

$$S(r) = M(1-\alpha e^{-\gamma r}) \qquad (4)$$

for the scatter-radius function was reported. Although expression (4) is simpler than the original Meredith-Neary representation using Bessel functions, it nevertheless leads to rather complex scatter integrals and a Wheatley optical

integrator (1951) has therefore been constructed to speed evaluation.

The integrator (Fig. 14) uses an opaque mask in which is a transparent sector whose area between radii r and (r + dr) is proportional to the integral of (4) between the same two radii. The mask is spun in front of a stationary cut-out whose shape is the same as that of the radiation field under study; the mask pivots about the point in the field at which the scattered intensity is desired. A photocell-galvanometer arrangement integrates the light transmitted during one revolution by the combined stationary and moving cut-outs, giving a signal proportional to the required intensity.

A modification of the apparatus, which will allow the pivot point of the rotating mask to be driven continuously across the field cut-out while the galvanometer output is simultaneously recorded, is under construction. This arrangement permits the variation of scattered intensity across any chord of the field to be plotted automatically.

BIBLIOGRAPHY

Balkwell, W. R. and Adams, G. D.: Rad. Res., 12 (4), 419 (1960)

Bouziques, H., Scheidhauer, J., and Brian, R.: "Selected topics in radiation dosimetry" P. 331, IAEA (Vienna) 1961

Burrus, W. R.: ORNL-3743 (1965)

Burrus, W. R. and Verbinski, V.V.: USAEC-U.S. Army, NDL-23-63 (1963)

Day, M. J., Stein, J. and Weiss, J.: Nature, 161, 650 (1948) and 164, 671 (1949)

Fortune, W. B., and Mellon, M.G.: Ind. Eng. Chem., 10 (60) 1938

BIBLIOGRAPHY (Cont'd)

Gibbs, H. D.	J. Biol. Chem., 72, 649 (1927)
Hubbel, J. H. and Scofield, N.E.	IRE Trans. NS-5, 156 (1958)
Johnson, T.R. and Martin, J.J.	Nucleonics, 20 (1), 83 (1962)
Klein, N.	Health Physics, 6, 212 (1961)
Sinclair, W.K.	Nucleonics, 7(6), 21 (1950)
Stahel, E.	Strahlenth., 31, 58 (1929)
VanDilla, M.A.	Ph.D. Thesis, M.I.T. (1951)
Whyte, G.N.	"Principles of Radiation Dosimetry", P. 111; Wiley (New York), 1959
Yoe, J.H. and Armstrong, J.	Ind. Eng. Chem., 16(2), 111 (1944)

MISCELLANEOUS

An account of the spectrometric work was presented at the Congress of the International Organization for Medical Physics, held in September 1965 at Harrogate, England.

It is proposed to present further results at the Radiological Society of North America meeting to be held in Chicago, Illinois, December 1966.

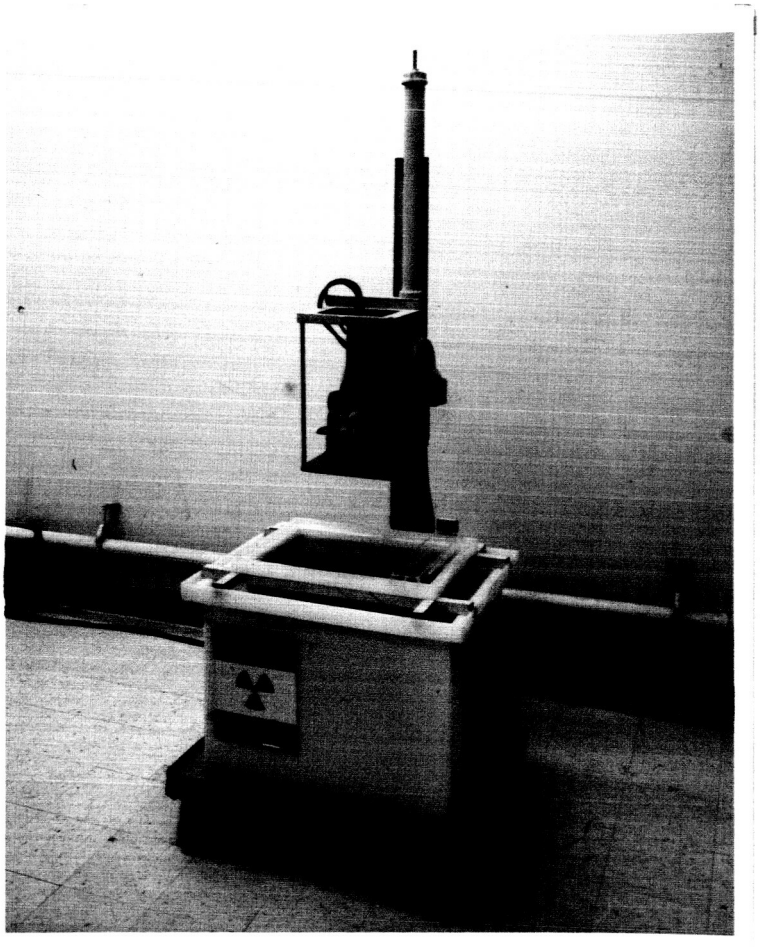

Fig. 1

Slab phantom, with scintillation detector used in estimating photon spectra

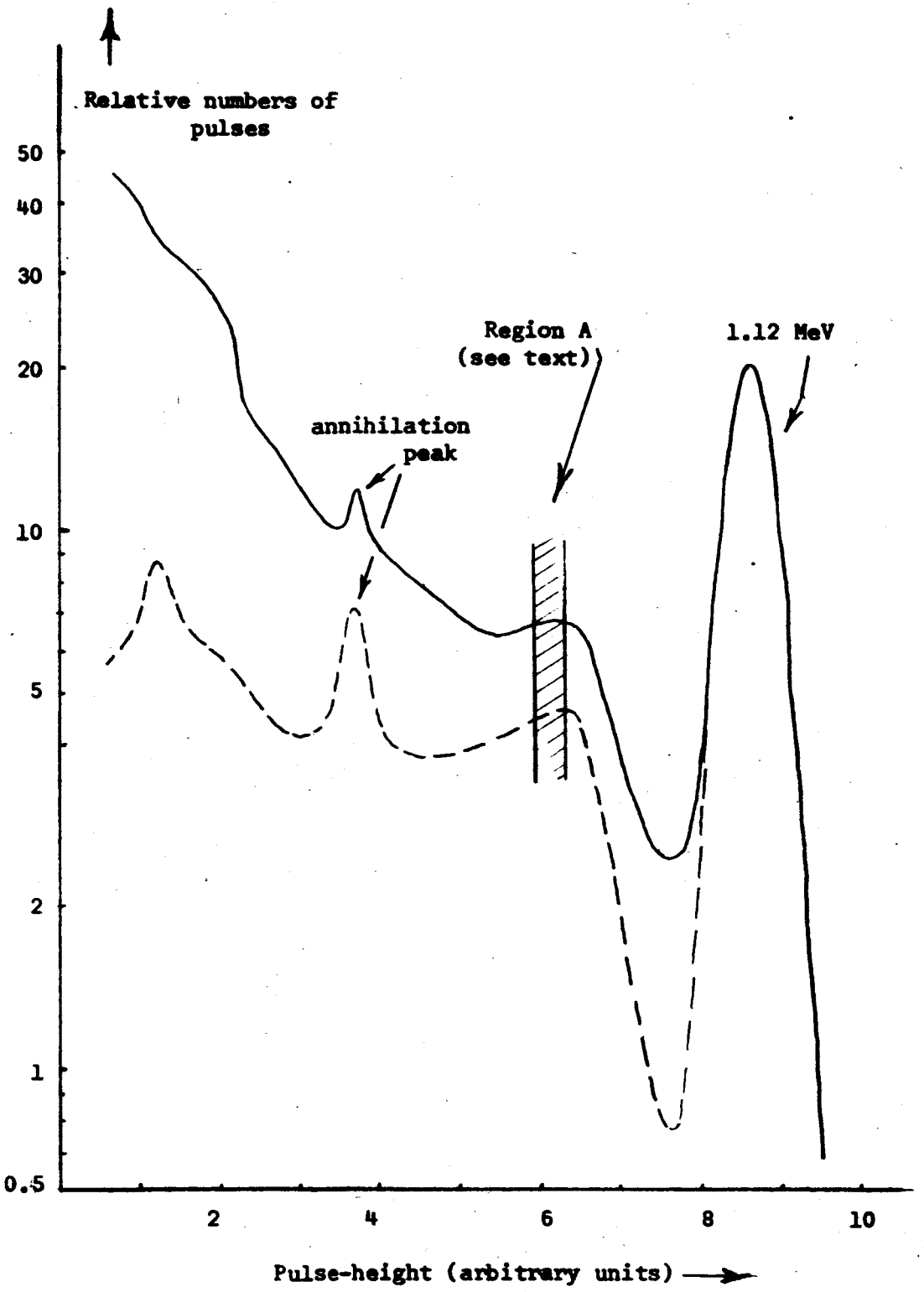

Fig.2 : Pulse-height spectra obtained from scatter-free (broken curve) and thick (solid line) Zn 65 sources.

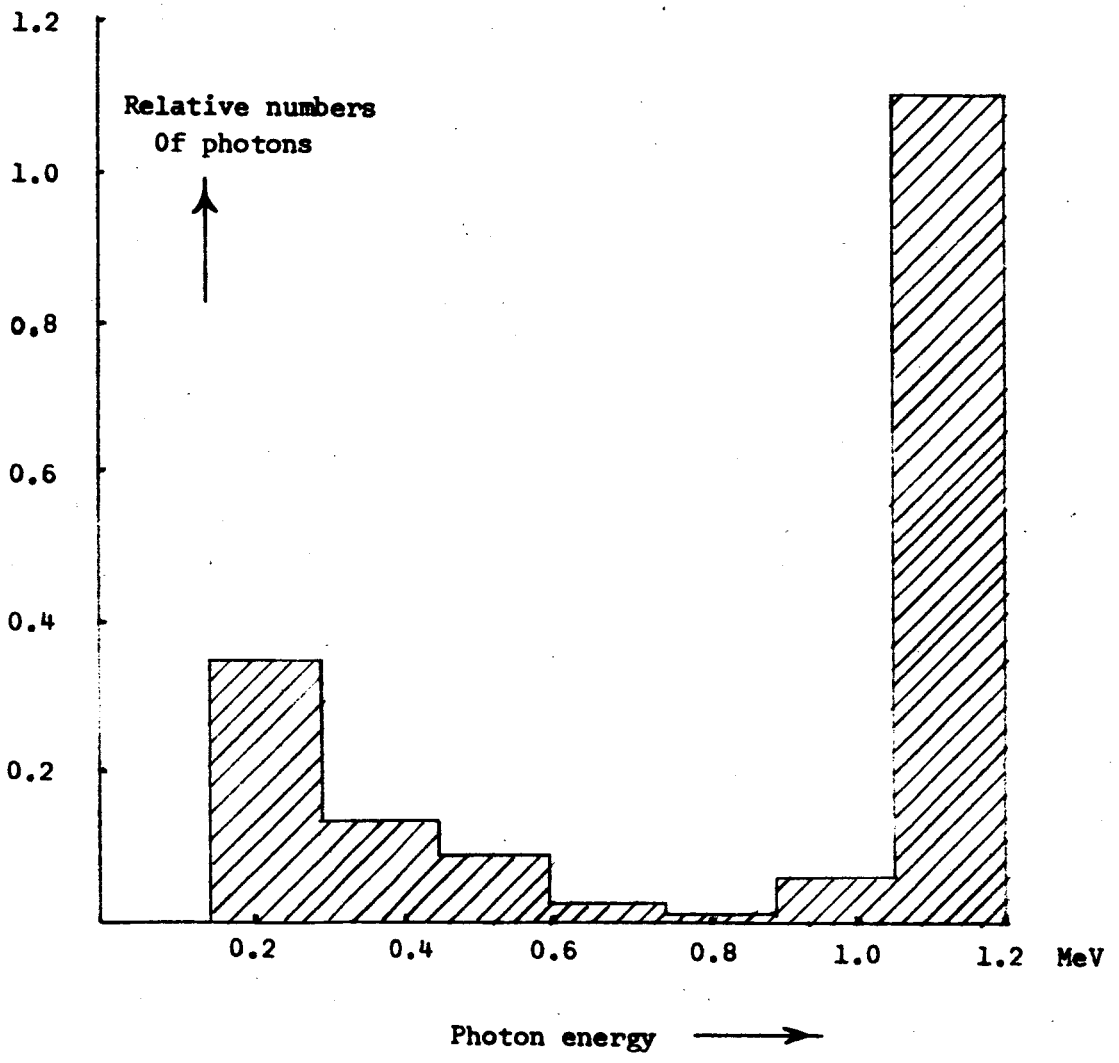

Fig. 3: Photon spectrum obtained with 8 x 8 unscrambling matrix

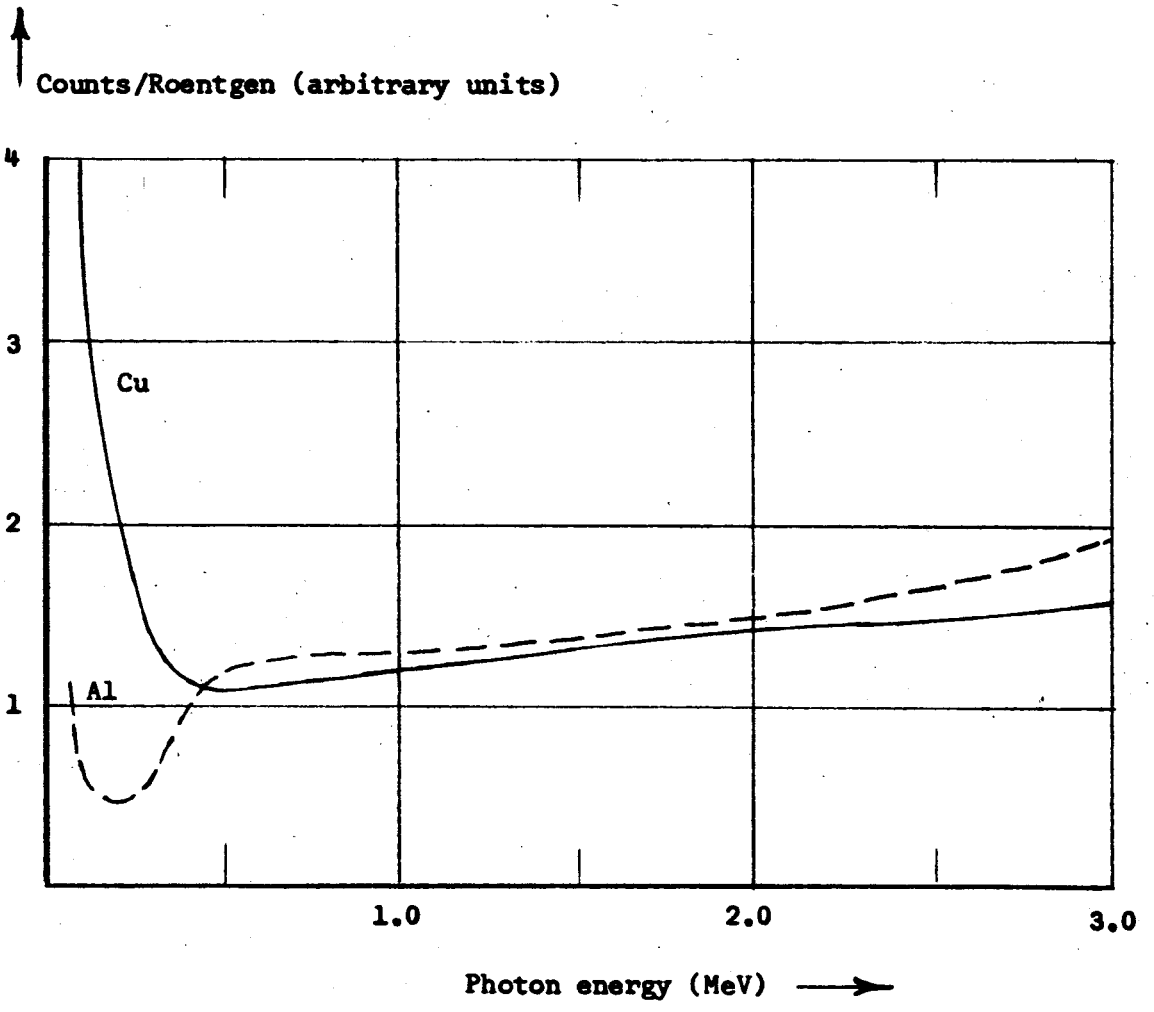

Fig. 4

Response of Geiger-Müller counters with aluminum (dashed curve) and copper (solid curve) cathodes. After Sinclair (1950).

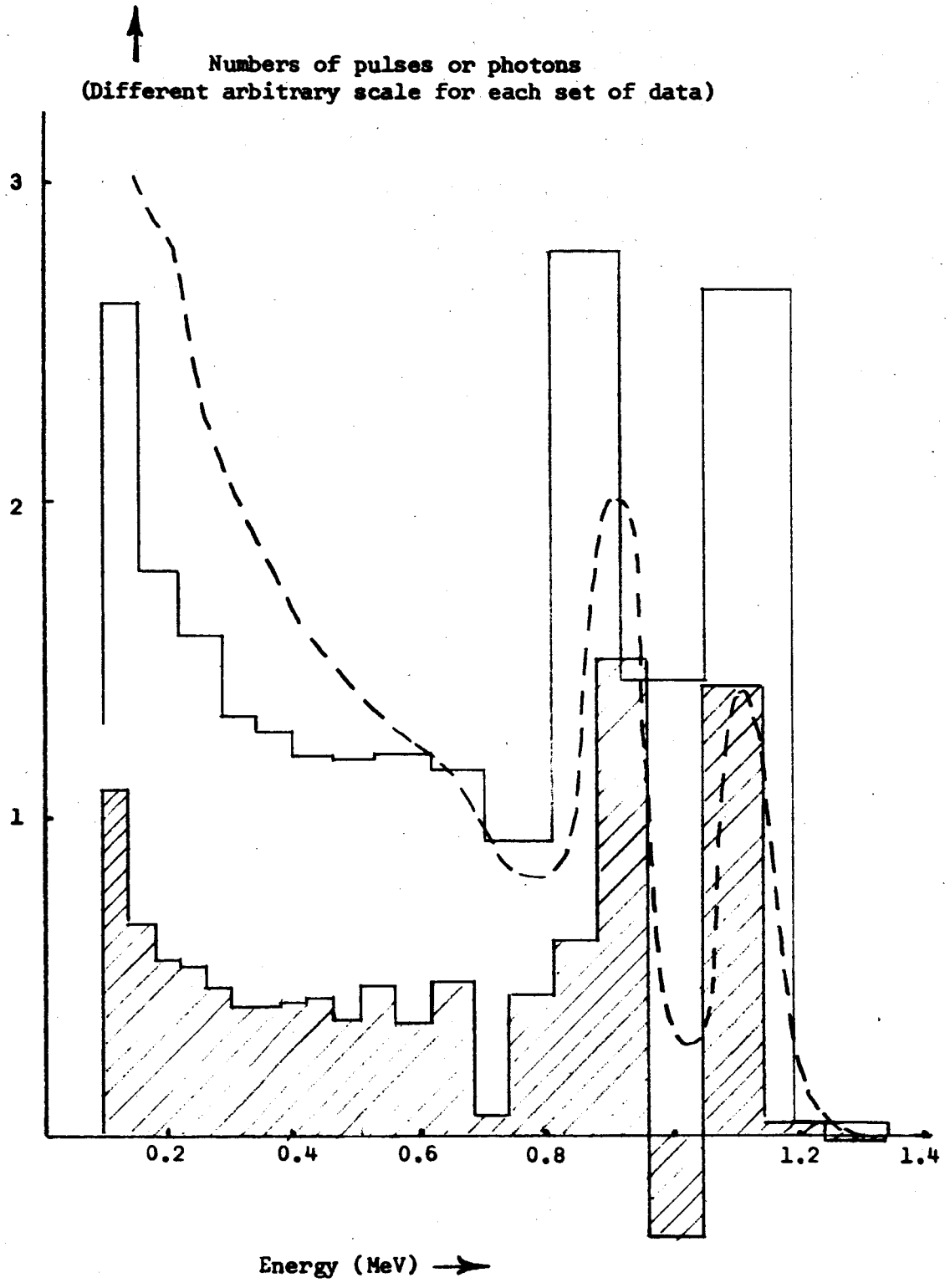

Fig. 5

Pulse-height spectrum (broken curve) obtained from Sc^{46} under scattering conditions, with photon spectrum (unshaded histogram) obtained by unscrambling with 14 x 14 matrix; the shaded histogram was obtained by using a 21 x 21 array.

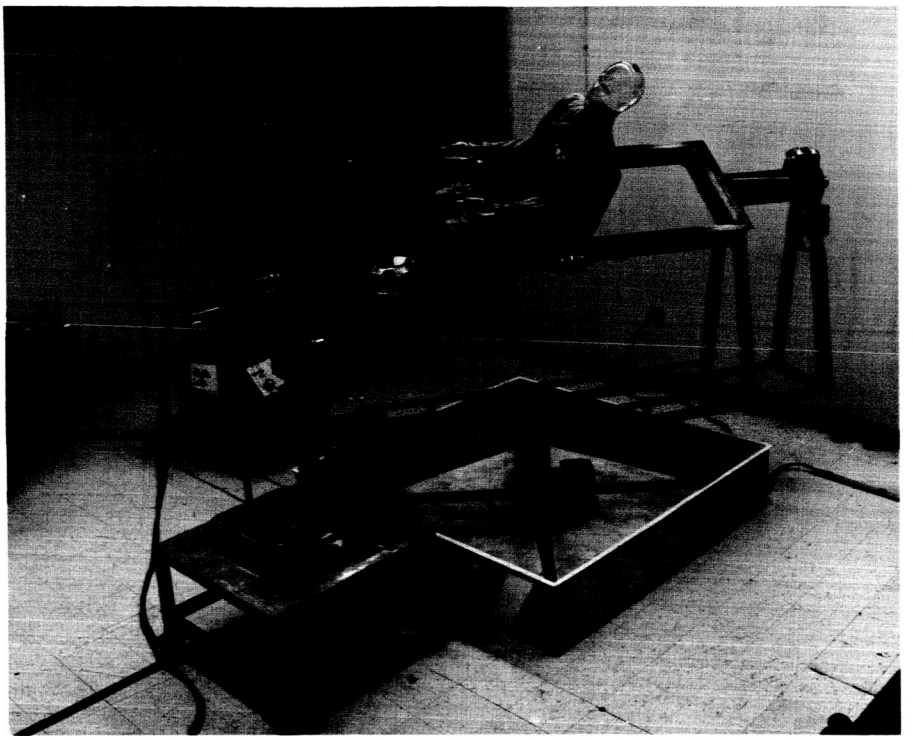

Fig. 6

General view of phantom system

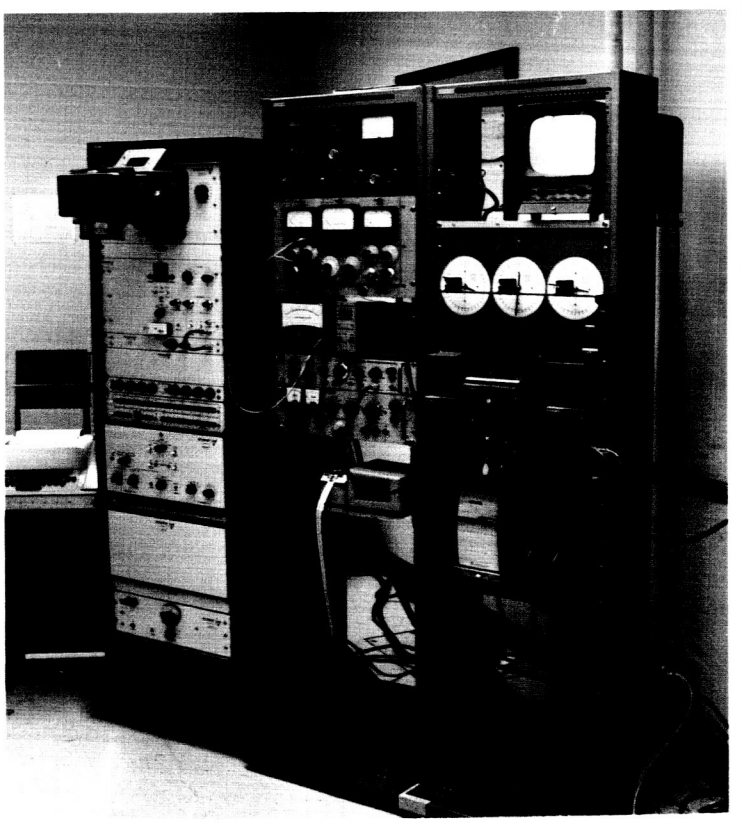

Fig. 7

Multichannel analyzer and phantom control system

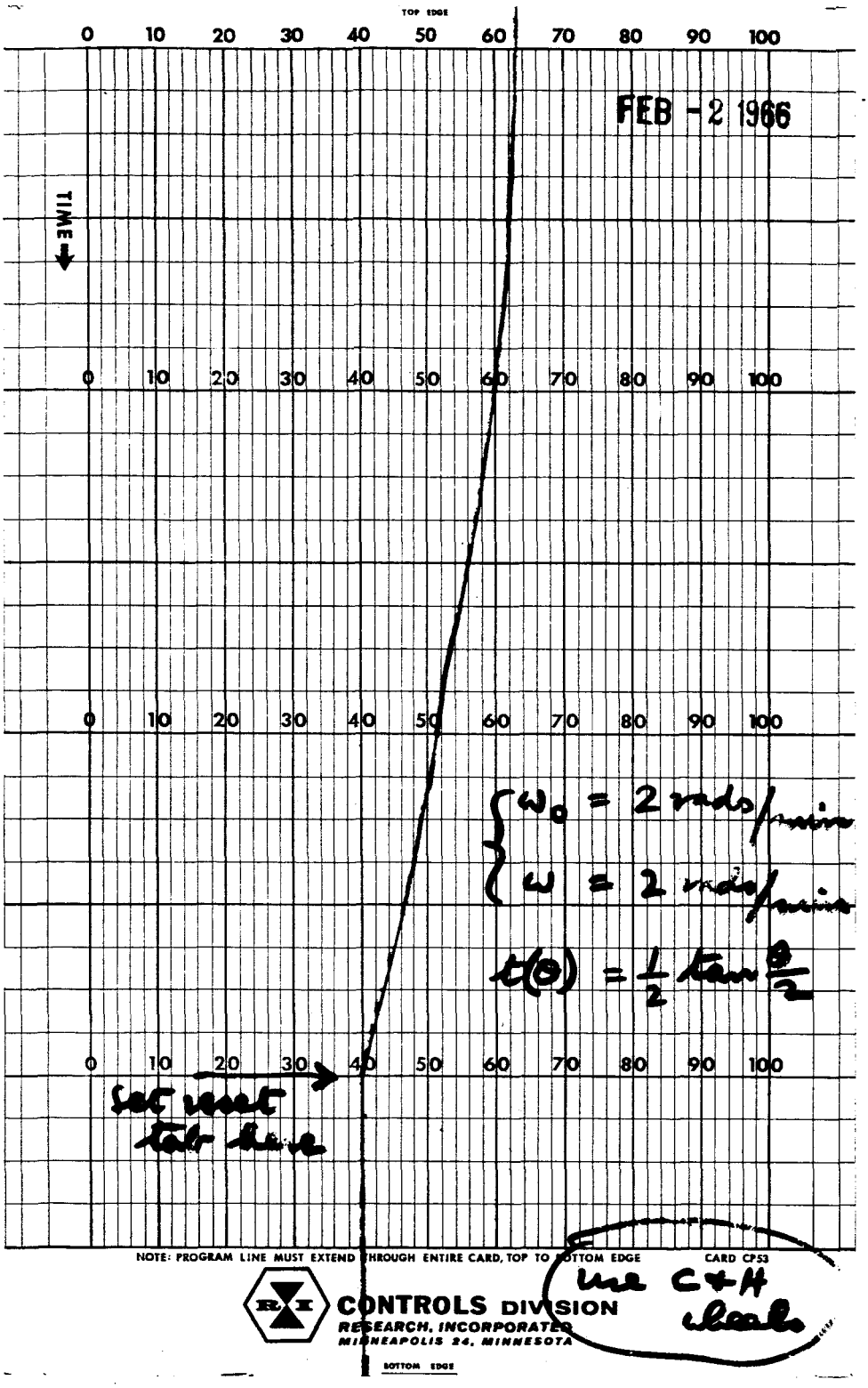

Fig. 8

Typical control program in which the required motor speed setting (horizontal axis) is plotted as a function of time (vertical axis, time increasing downwards). The program line, which is a graved mark, has been inked in here for clarity.

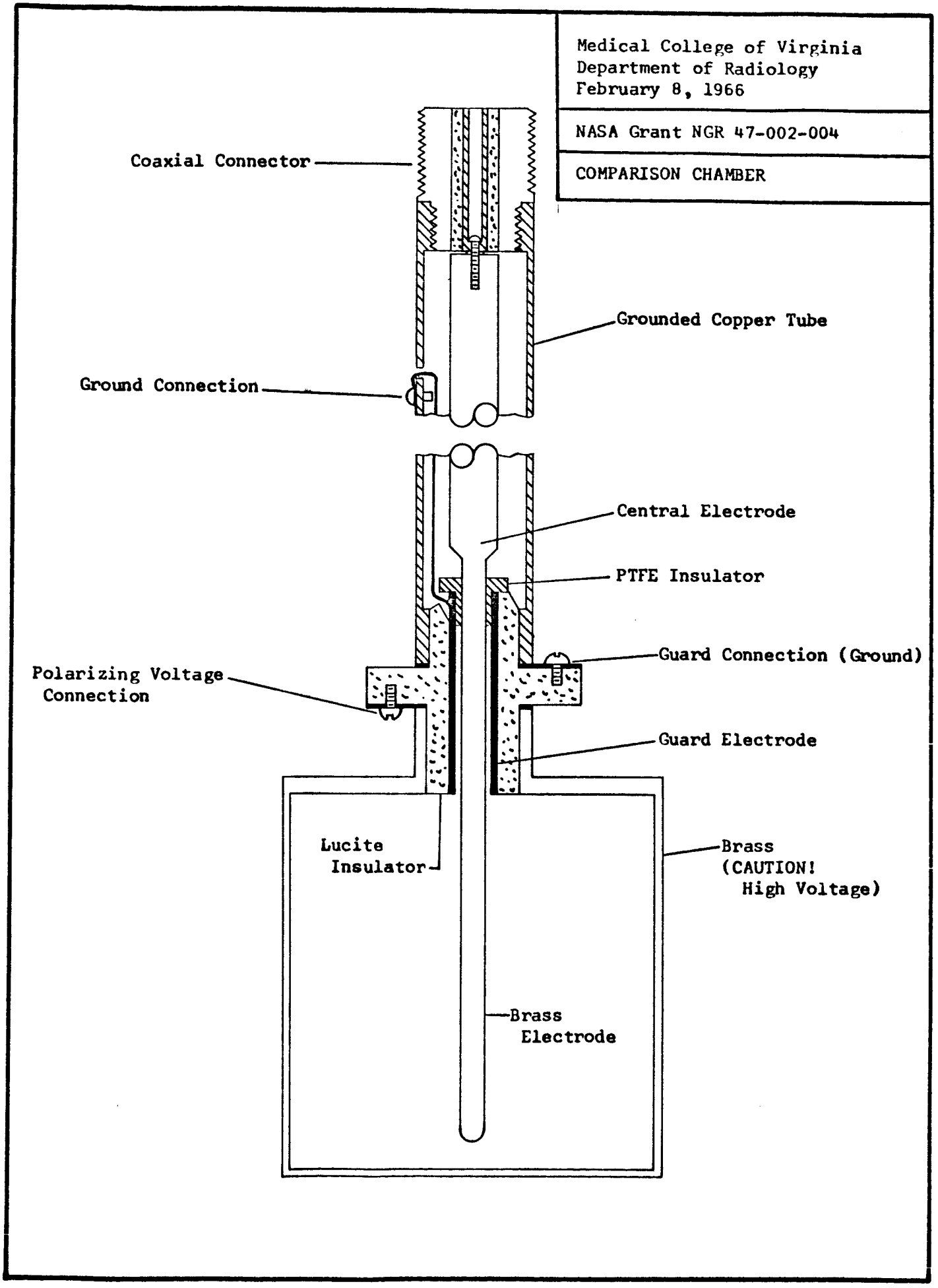
Medical College of Virginia
Department of Radiology
February 8, 1966
NASA Grant NGR 47-002-004
COMPARISON CHAMBER
Coaxial Connector
Grounded Copper Tube
Ground Connection
Central Electrode
PTFE Insulator
Guard Connection (Ground)
Polarizing Voltage Connection
Guard Electrode
Lucite Insulator
Brass (CAUTION! High Voltage)
Brass Electrode

Fig. 9

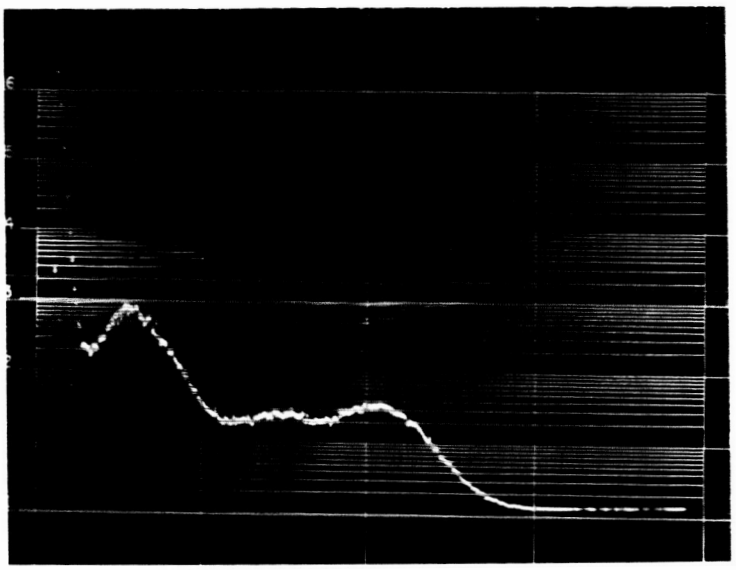

Fig. 10(a)

Signal (background subtracted) from 0.513 MeV Sr^{85} gamma-rays, incident on anthracene crystal. The scale (despite the graticule) is linear vertically, as well as horizontally.

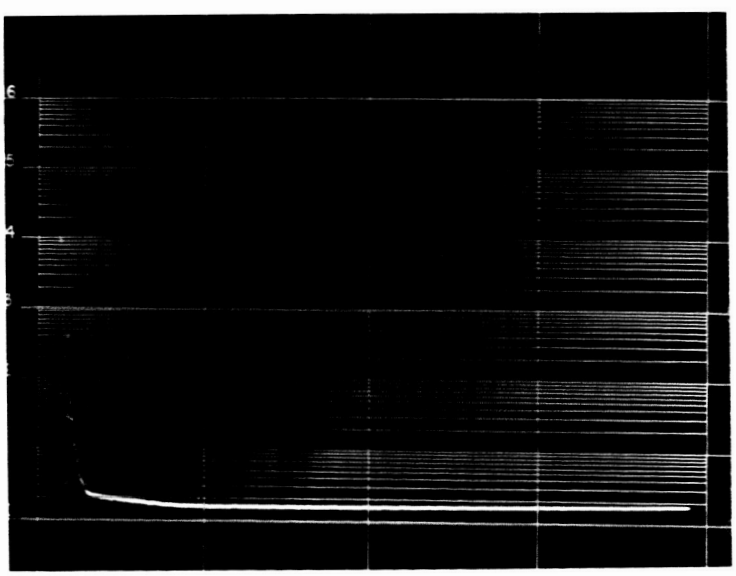

Fig. 10(b)

Background which was subtracted from spectrum of Fig. 10(a).

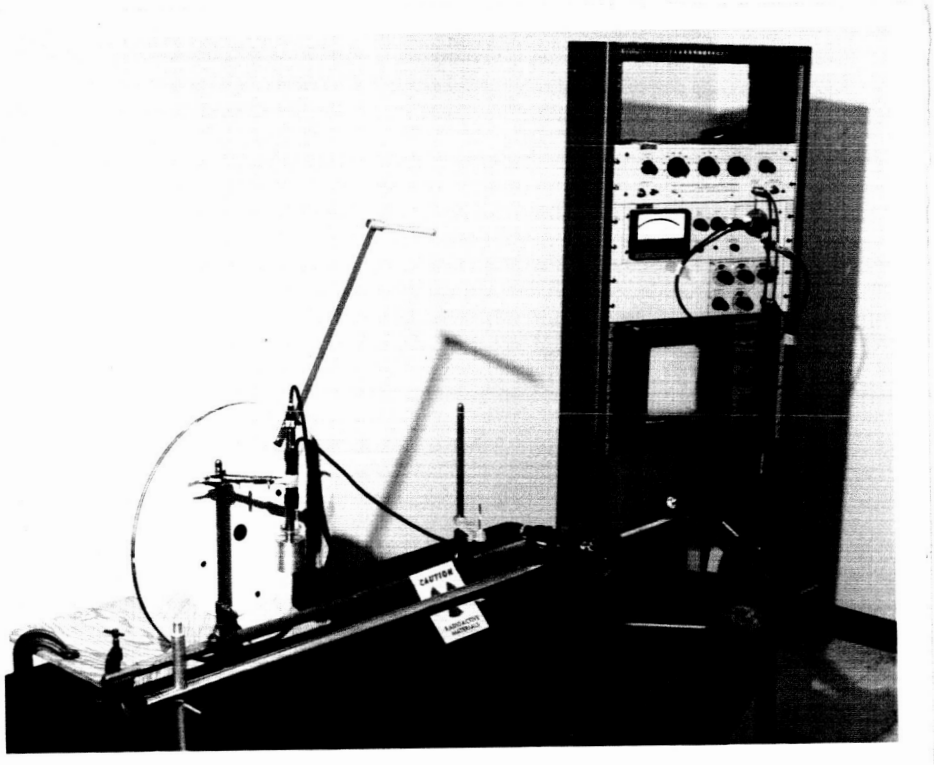

Fig. 11

Calibration set-up for E-detectors. In practice both the horizontal cathetometer and the electrometer system are at a considerable distance from the source, to minimize observer exposure. The circular board is used in measuring angular sensitivity-dependence.

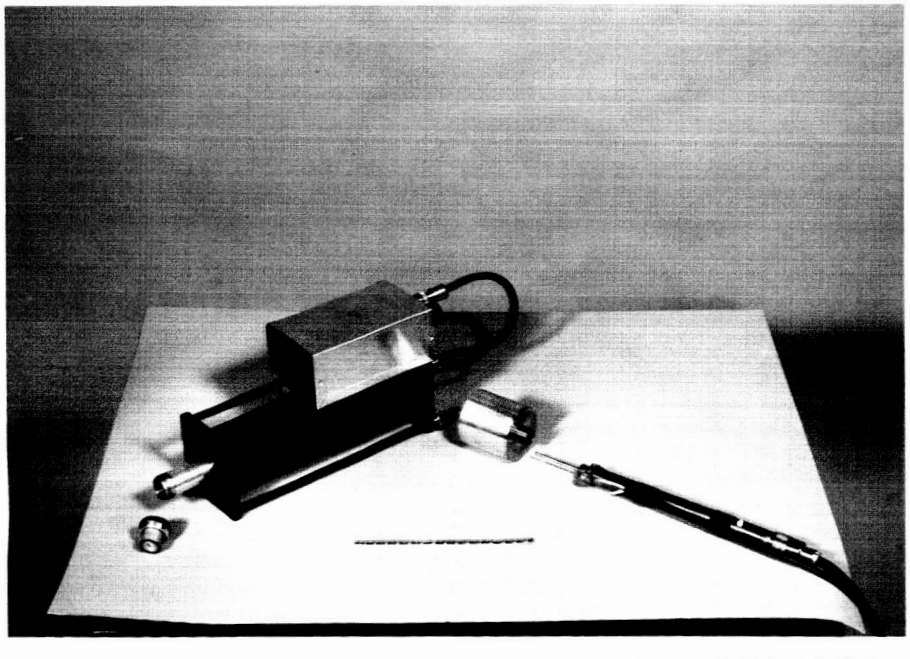

Fig. 12

Anthracene detector (left, with crystal removed) and comparison chamber (right, partly disassembled).

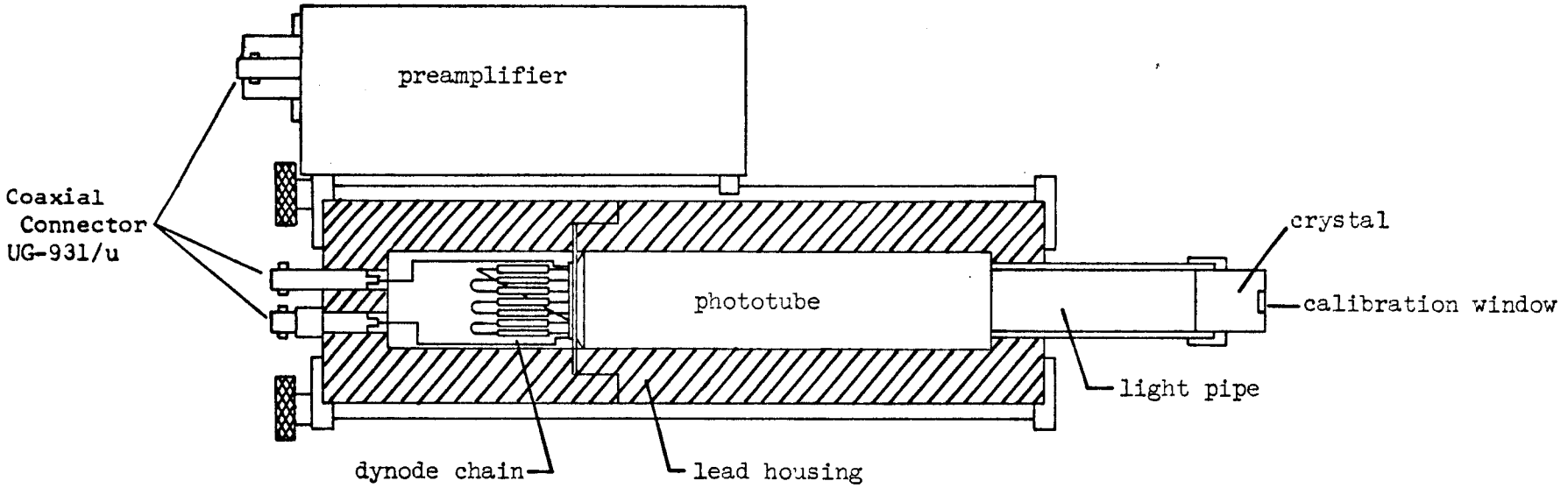

ANTHRACENE DETECTOR

Medical College of Virginia Department of Radiology February 11, 1966
NASA Grant NGR 47-002-004
ANTHRACENE DETECTOR

Fig. 13

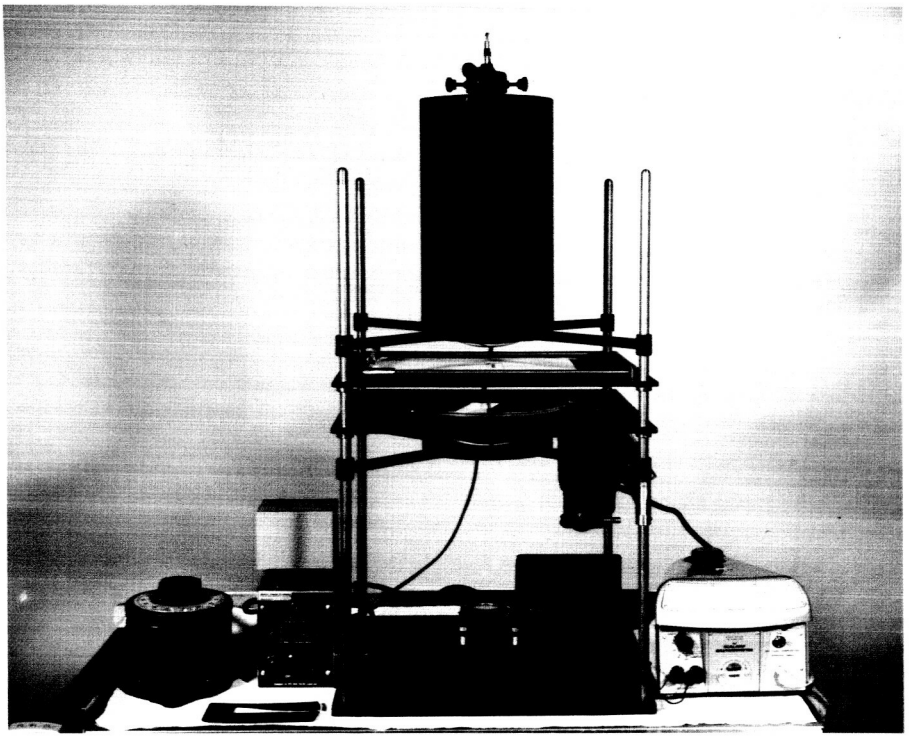

Fig. 14

The Wheatley integrator. From the top downwards can be seen the lamp housing, first condenser lens, field mask (here a triangle) rotating sector mount, second condenser lens, photocell; the readout galvanometer is on the right, the lamp brightness and motor speed controls on the left.